Science in China Series F: Information Sciences

www.scichina.com
info.scichina.com
www.springer.com/scp
www.springerlink.com

Characteristic model based control of the X-34 reusable launch vehicle in its climbing phase

MENG Bin[1†], WU HongXin[1], LIN ZongLi[2] & LI Guo[1]

[1] National Laboratory of Space Intelligent Control, Beijing Institute of Control Engineering, Beijing 100190, China;
[2] Charles L. Brown Department of Electrical and Computer Engineering, University of Virginia, Charlottesville, VA 22904-4743, USA

In this paper, a characteristic model based longitudinal control design for the trans-aerosphere vehicle X-34 in its transonic and hypersonic climbing phase is proposed. The design is based on the dynamic characteristics of the vehicle and the curves it is to track in this climbing phase. Through a detailed analysis of the aerodynamics and vehicle dynamics during this climbing phase, an explicit description of the tracking curve for the flight path angle is derived. On the basis of this tracking curve, the tracking curves for the two short-period variables, the angle of attack and the pitch rate, are designed. An all-coefficient adaptive controller is then designed, based on the characteristic modeling, to cause these two short-period variables to follow their respective tracking curves. The proposed design does not require multiple working points, making the design procedure simple. Numerical simulation is performed to validate the performance of the controller. The simulation results indicate that the resulting control law ensures that the vehicle climbs up successfully under the restrictions on the pitch angle and overloading.

trans-aerosphere vehicle X-34, climbing phase, characteristic modeling, adaptive control, robustness

1 Introduction

The X-34, designed and built by the Orbital Sciences Corporation, is an unmanned sub-orbital vehicle designed for use as a flight test bed to demonstrate key vehicle and operational technologies applicable to future reusable launch vehicles. The X-34 is to be air-launched from an L-1011 carrier aircraft at approximately a Mach number of 0.7 and an altitude of 11 km, where an onboard engine will accelerate the vehicle to speeds above Mach 8 and an altitude of 80 km. An un-powered entry will follow, leading to an autonomous landing. When claiming in the atmosphere, the trans-atmosphere vehicle usually experiences a very quick climbing process with sharp changes in its speed and altitude due to the immense engine power, frequently causing the aerodynamic characteristics, lift efficiency and helm efficiency of the vehicle to change rapidly. In the mean time, a large amount of fuel has to be carried by the vehicle and will be rapidly consumed in the climbing process. This results in the rapid changes in the weight, center of gravity and moment of inertia of the vehicle. All these

Received January 5, 2009; accepted August 7, 2009
doi: 10.1007/s11432-009-0182-x
†Corresponding author (email: mengb@amss.ac.cn)
Supported in part by the National Natural Science Foundation of China (Grant Nos. 90405017, 60736023, 60704014), in part by China Postdoctoral Funds (Grant No. 20060400415), and in part by a Cheung Kong Professorship at Shanghai Jiao Tong University

Citation: Meng B, Wu H X, Lin Z L, et al. Characteristic model based control of the X-34 reusable launch vehicle in its climbing phase. Sci China Ser F-Inf Sci, 2009, 52(11): 2216–2225, doi: 10.1007/s11432-009-0182-x

changes will affect the steering stability and the dynamic responses of the vehicle considerably[1−3].

In this paper we are concerned with the characteristic analysis and control law design for the trans-atmosphere vehicle X-34 in the high altitude and high speed climbing phase (from Mach 2.5 to Mach 7.2). This is different from the control of ordinary aircraft due to the extremely low air density in the high altitude. An analysis of the vehicle dynamics and various aerodynamic data indicates that several difficulties arise in carrying out such a task. 1) After the powered and un-powered ascending in the climbing phase, the altitude is required to be higher than a predetermined value imposed by the surface thermal insulation material property and the speed is constrained by the vehicle structural property. Thus the coordination between the altitude and the speed is a challenge. 2) A close examination of the dynamic model of the vehicle reveals that the air dynamic pressure, as the control coefficient of the speed and the flight path angle, decreases rapidly as the air density decreases rapidly during the high altitude and high speed climbing phase, making these two long-period variables hard to control. 3) The climbing control of the vehicle will have to be achieved by appropriate control of the short-period variables. 4) The rapid changes of the aerodynamic characteristics in the climbing phase, in a strong nonlinear fashion, make it extremely difficult to identify the aerodynamic parameters and the consequent analytic expression of the dynamic, which are crucial for modern control designs.

There have been few papers on the climbing control of trans-atmosphere vehicles. In ref. [3], the authors investigated the control problems under the flight conditions of Mach 0–4 and altitude of 0–40 km. Using classical control approaches, the climbing objective is achieved by selecting different working points, designing inner and outer loop PID control laws, and parameter tuning. However, the authors did not describe the method for designing the tracking curves.

The objective of this paper is to investigate the characteristics of the trans-atmosphere vehicle X-34 in the climbing phase at the supersonic and hypersonic speeds (from Mach 2.5 to Mach 7.2) and to design the tracking curves and the longitudinal control laws. By a careful analysis of the aerodynamic data and the vehicle dynamics in the high altitude and high speed climbing phase, we propose a method for designing the flight path angle tracking curve and draw the conclusion that the long-period variables cannot be directly controlled in this phase, laying the foundation of our climbing control design. More specifically, based on these results, we design the tracking curves for the angle of attack and the pitch rate and a characteristic model based all-coefficient adaptive control law for these two short-period variables. A salient feature of our control design is that it does not require multiple working points, which significantly simplifies the design process. Simulation results show that our design achieves the climbing objective under the constraints on the pitch angle and overload.

Characteristic model based all-coefficient adaptive control was proposed by Wu[4,5] in 1980s. Significant progresses in both theories and applications as well as its integration with adaptive control design have been made in the past two decades[4−9]. The characteristic model based all-coefficient adaptive control is aimed at designing engineering-oriented adaptive control, which does not depend on the explicit dynamic model of the system and requires to identify and adapt only a few parameters. Such an approach can guarantee the transient performance of the closed-loop system and hence overcome the practical difficulties in the implementation of adaptive control laws[8]. Many successful applications of the characteristic model based all-coefficient adaptive control have been found in various industries. In particular, its application in the reentry adaptive control of a manned spaceship achieves an accuracy of the parachute-opening point that is among the most accurate[6].

The remainder of the paper is organized as follows. Section 2 recalls some preliminaries and describes the problem to be solved in the paper. Section 3 describes the design of tracking curves. Section 4 presents the design of the control law. Section 5 includes the simulation results. Section 6 draws a brief conclusion to the paper. The nomenclature used in the paper is listed in Appendix.

2 Preliminaries and problem description

We will investigate the characteristic model based climbing control design for the trans-atmosphere vehicle X-34. In this section, we will first briefly describe the operation of the vehicle, its control input, its dynamic model and the aerodynamic modeling. We will then review the characteristic model based all-coefficient adaptive control method. Finally, we will describe the climbing control problem we are to solve in this paper.

2.1 The trans-aerosphere vehicle X-34

As detailed in refs. [1, 2], the X-34 is an unmanned sub-orbital vehicle designed to be used as a flight test bed to demonstrate key vehicle and operational technologies applicable to future reusable launch vehicles. The X-34 is to be air-launched from an L-1011 carrier aircraft at approximately Mach 0.7 and an altitude of 11 km, where an onboard engine will accelerate the vehicle to speeds above Mach 8 and an altitude of 80 km. An un-powered entry and landing will follow. The X-34 will be powered by a "Fastrac" rocket engine, which is designed for a nominal thrust of 240 kN and is expected to have a thrust vectoring capability of $\pm 15°$ in the pitching plane. The aerodynamic control surfaces are elevons, a body flap, an all-moving vertical tail, and a tail-mounted speed brake. The amplitude and change rate of the elevons are constrained within -30–20 degrees and $\pm 60°$/s, respectively. The vehicle also features reaction control system (RCS) for roll and yaw control. The aerodynamic parameters and the descriptions of the rapid changes of the center of gravity, mass and moment of inertia are all from refs. [1, 2]. The rotation of the earth has to be taken into account in modeling vehicles at speeds higher than Mach 3. We adopt the WGS84 model for the earth and acceleration of gravity[10], which takes into account the differences among various sea levels at different places, in constructing our simulation model for the vehicle at hypersonic speeds. The longitudinal dynamics of the vehicle is represented by[11]

$$\dot{V} = -\frac{\mu}{r^2}\sin\gamma + \frac{P\cos\alpha - D}{m} + \omega_E^2 r\sin\gamma, \quad (1)$$

$$\dot{\gamma} = -\left(\frac{\mu}{Vr^2} - \frac{V}{r}\right)\cos\gamma + \frac{P\sin\alpha + L}{mV} + 2\omega_E + \frac{\omega_E^2 r\cos\gamma}{V}, \quad (2)$$

$$\dot{h} = V\sin\gamma, \quad (3)$$

$$\dot{q} = \frac{M_y}{I_y}, \quad (4)$$

$$\dot{\alpha} = q - \dot{\gamma}, \quad (5)$$

where the variables V, γ, h, q and α are respectively the velocity, flight path angle, altitude, pitch rate and angle of attack of the vehicle, L, D and M_y are respectively the lift, drag and pitching moment defined as

$$L = \frac{1}{2}\rho V^2 S C_L,$$
$$D = \frac{1}{2}\rho V^2 S C_D,$$
$$M_y = \frac{1}{2}\rho V^2 S\bar{c} C_M,$$

C_L, C_D, C_M and C_Z are respectively lift coefficient, drag coefficient, pitching moment coefficient, and the total aerodynamic coefficient in the Z direction of the body coordinate system and are defined as

$$C_L = \overline{CLB} + \overline{CLDE} + \overline{CLBF},$$
$$C_D = \overline{CDB} + \overline{CDDE} + \overline{CDBF},$$
$$C_Z = -C_L\cos\alpha - C_D\sin\alpha,$$
$$C_M = \overline{CMB} + \overline{CMDE} + \overline{CMBF} + \frac{\bar{c}q}{2V}\overline{CMQ} - \frac{C_Z(\overline{XCG} - \overline{CGREF})}{\bar{c}},$$

$r = h + R_E$, and finally the parameters μ, ω_E, m, P, I_y, ρ, S, $\bar{c}$, R_E, $\overline{CLB}$, $\overline{CLDE}$, $\overline{CLBF}$, $\overline{CDB}$, $\overline{CDDE}$, $\overline{CDBF}$, $\overline{CMB}$, $\overline{CMDE}$, $\overline{CMBF}$, $\overline{CMQ}$, $\overline{XCG}$ and $\overline{CGREF}$ are as defined in Appendix.

2.2 Characteristic model based all-coefficient adaptive control

In the design of a characteristic model based all-coefficient adaptive control law, a characteristic model of the plant to be controlled is first established, and based on this characteristic model, all-coefficient adaptive control is designed.

2.2.1 The characteristic model. The key idea of the characteristic modeling is to model the plant based not only on the dynamic characteristics of the plant but also on the control performance requirements. A characteristic model has the following important features. 1) Same input leads to same output for the plant and its characteristic model. 2) The specific form and the order of a characteristic model mainly rely on the control performance requirements. 3) The structure of a characteristic model is simpler than that of its original dynamic equations, and thus is more convenient in engineering applications. 4) It is essentially different from the conventional reduced-order model, and it compresses the information of the system dynamics into several characteristic variables. Within the bandwidth of the control system, no information is lost.

According to the requirements of the control problem at hand, the characteristic model for each variable of the X-34 vehicle is described by the following time-varying difference equation:

$$\begin{aligned} y(k+1) = f_1(k)y(k) + f_2(k)y(k-1) \\ + f_3(k)u(k), \end{aligned} \tag{6}$$

where $u(k)$ and $y(k)$ denote respectively the input and output of the system, and the time-varying coefficients $f_1(k)$, $f_2(k)$ and $f_3(k)$ belong to the convex set

$$\begin{aligned} D_s = \left\{ \begin{pmatrix} f_1 \\ f_2 \\ f_3 \end{pmatrix} \in \mathbb{R}^3 : 1.4331 \leqslant f_1 \leqslant 1.9974, \right. \\ -0.9999 \leqslant f_2 \leqslant -0.5134, \\ 0.9196 \leqslant f_1 + f_2 \leqslant 0.9999, \\ \left. 0.003 \leqslant f_3 \leqslant 0.3 \right\}, \end{aligned} \tag{7}$$

which was derived in ref. [12].

2.2.2 Parameter identification. The coefficients of a characteristic model are constrained to certain ranges. This is a key feature of the characteristic model based all-coefficient adaptive control design. It is reasonable, and necessary indeed, in any engineering application to impose constraints on system and design parameters. In our application in hand, we will use the weighted least squares method to identify the parameters f_1, f_2 and f_3 and then map them onto the convex set D_s. Denote the mapped images by $\hat{f}_1$, $\hat{f}_2$ and $\hat{f}_3$, respectively. Here we adopt a direct mapping approach. If the identification result dose not belong to the convex set D_s, then $\hat{f}_1$, $\hat{f}_2$ and $\hat{f}_3$ take values corresponding to the boundary point of D_s that has the shortest distance from the point corresponding to the identified results.

2.2.3 All-coefficient adaptive control and its stability. The characteristic model based all-coefficient adaptive control can be designed as follows:

$$u(k) = u_0(k) + u_{\mathrm{G}}(k) + u_{\mathrm{I}}(k) + u_{\mathrm{D}}(k), \tag{8}$$

where $u_0(k)$, $u_{\mathrm{G}}(k)$, $u_{\mathrm{I}}(k)$ and $u_{\mathrm{D}}(k)$ are respectively referred to as the tracking controller, the golden-section controller, the logic integral controller and the logic differential controller and are given by

$$\begin{aligned} u_0(k) &= \frac{y_{\mathrm{R}}(k+1) - \hat{f}_1(k)y_{\mathrm{R}}(k) - \hat{f}_2(k)y_{\mathrm{R}}(k-1)}{\hat{f}_3(k)}, \\ u_{\mathrm{G}}(k) &= -\frac{l_1\hat{f}_1(k)e(k) + l_2\hat{f}_2(k)e(k-1)}{\hat{f}_3(k)}, \\ u_{\mathrm{I}}(k) &= u_{\mathrm{I}}(k-1) - k_{\mathrm{I}}e(k), \\ u_{\mathrm{D}}(k) &= -k_{\mathrm{D}}e(k), \end{aligned}$$

$e(k) = y(k) - y_{\mathrm{R}}(k)$, $y_{\mathrm{R}}(k)$ is the tracking target function, $l_1 = 0.382$, $l_2 = 0.618$,

$$k_{\mathrm{I}} = \begin{cases} k_{\mathrm{I}1}, & \text{if } e(k)(e(k) - e(k-1)) > 0, \\ k_{\mathrm{I}2}, & \text{if } e(k)(e(k) - e(k-1)) \leqslant 0, \end{cases}$$

$$k_{\mathrm{D}} = c_{\mathrm{D}}\sqrt{\sum_{j=0}^{l_{\mathrm{D}}} |e(k)|} \left(\text{or } c_{\mathrm{D}}\sqrt{\sum_{j=0}^{l_{\mathrm{D}}} e^2(k)} \right),$$

and finally, $k_{\mathrm{I}1} \gg k_{\mathrm{I}2} > 0$, $c_{\mathrm{D}} > 0$, $l_{\mathrm{D}} > 0$ are constants.

It is proven in ref. [9] that this adaptive controller guarantees the transient property and the robust stability of the resulting closed-loop system. It is easy to tell that all-coefficient adaptive control is essentially different from conventional adaptive control in that the identified parameters are the coefficients of the characteristic model and are independent of the forms of unknown parameters of the system dynamics. As a result, the constraints on the forms of the unknown parameters in the nonlinear adaptive control diminish.

2.3 Problem formulation: climbing control of the X-34 vehicle

We consider in this paper the design of a longitudinal climbing controller for the trans-atmosphere vehicle X-34. A detailed analysis of various vehicle dynamics and aerodynamics data during the climbing process shows that the high altitude and high speed climbing phase of 25 km (Mach 2.5) to 72 km (Mach 7.2) is different from that of 7 km (Mach 0.7) to 25 km (March 2.5). Its control strategy is also different from that of conventional aerial vehicles. According to refs. [1, 2], a typical flight trajectory of the X-34 is given by

$$h(t) = 10M(t), \quad t \leqslant 200 \text{ s}, \tag{9}$$

where $h(t)$ is the altitude (in km) of the vehicle at time t (in second), $M(t)$ is the speed (in Mach number) of the vehicle at time t, $h(t_0) = 25$ km, $M(t_0) = 2.5$ Mach, $h(200) = 72$ km, $M(200) = 7.2$ Mach, and t_0 will be specified later. During the flight, the pitch angle is limited to below 35° and the overload is less than 2.

For simplicity in the design, the constant thrust is assumed to be in the direction of the body of the vehicle. An analysis of the aerodynamics indicates that the largest moment is obtained at −15° of body flap. The body flap is fixed at −15°. Physical limitations impose that the elevons are constrained within −30° and 20° in amplitude, and ±60°/s in rate.

3 Design of tracking curves

In this section, we derive the formula for calculating the tracking curve of the flight path angle. This is done by analyzing the dynamic model of the vehicle and various aerodynamic data. In doing so, a conclusion is drawn that the long-period variables, i.e., the speed and the flight path angle, are not directly controllable in the high altitude and high speed climbing phase. Based on these results, the tracking curves of the angle of attack and the pitch rate are designed.

3.1 Design of the speed tracking curve

By analyzing the data of μ/r^2, P/m and D/m in the dynamic model (1), the term D/m is found to be only approximately 1/50 of the other terms on the right-hand side of the equation when the angle of attack is within the range between 5° and 10° and the altitude is greater than 40 km (speed higher than Mach 4). That is, the control input hardly has any effect on the derivative of the speed. In other words, the speed is not directly controllable at a high altitude. At an altitude between 25 km (Mach 2.5) and 40 km (Mach 4), the term D/m assumes higher values, but is still negligible. Motivated by this observation, we will design the speed tracking curve backwards from time $t = 200$ s by curve fitting according to the open-loop characteristics of the vehicle to achieve the predetermined speed at $t = 200$ s. The resulting speed ascending curve is illustrated in Figure 1.

It is seen in Figure 1 that it takes 90 s for the speed to accelerate from Mach 2.5 to Mach 7.2. Therefore, the initial values in the our design are set as: the initial time when the engine starts is 110 s and the initial speed and altitude are Mach 2.5 and 25 km, respectively.

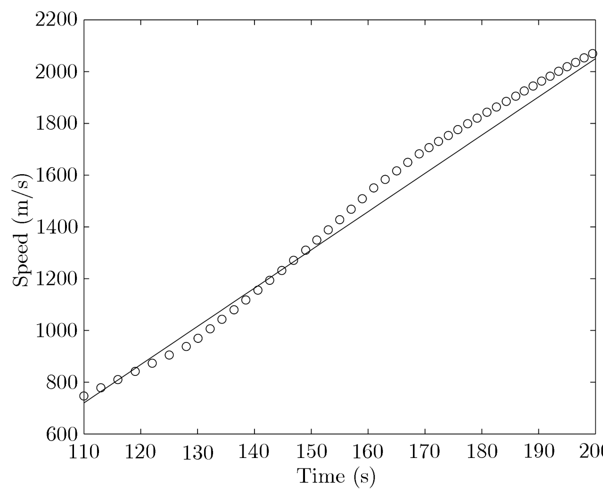

Figure 1 Comparison between the designed speed curve (in circled-line) and the straight speed ascending line (in solid line).

3.2 Design of the tracking curves of the altitude and the flight path angle

The altitude tracking curve is readily obtained from the control objective in (9) and Figure 1. We next consider the design of the tracking curve of the flight path angle γ by the dynamic model (3) and the tracking curve of the altitude.

When the altitude is higher than 40 km, the third term D/m on the right hand side of (1) can be neglected and, according to refs [1, 2], the angle of attack α is between 5° and 10°, for which $\cos\alpha$ approximately equals 1. Therefore, eq. (1) can be simplified to

$$\dot{V} = \frac{P}{m} - \frac{\mu}{r^2}\sin\gamma. \tag{10}$$

In view of the fact that the variation of the speed of sound a is far smaller than that of the vehicle speed, we assume a to be a constant for simplicity, that is,

$$M = \frac{V}{a},$$

from which we have

$$\dot{M} = \frac{\dot{V}}{a}.$$

Recalling that $h = 10M$, we have

$$\dot{h} = \frac{10\dot{V}}{a}.$$

In view of (3), that is,

$$\dot{h} = V\sin\gamma,$$

we have

$$\dot{V} = 10^{-1} \times aV\sin\gamma. \tag{11}$$

It then follows from (10) and (11) that

$$\frac{P}{m} = \left(\frac{\mu}{r^2} + 10^{-1} \times aV\right)\sin\gamma. \tag{12}$$

At an altitude between 25 and 40 km, the third term D/m in (1) is approximately 1 and can no longer be neglected; thus

$$\frac{P}{m} - 1 = \left(\frac{\mu}{r^2} + 10^{-1} \times aV\right)\sin\gamma. \tag{13}$$

The thrust in the climbing process is known. With given mass, speed and altitude of the vehicle, the tracking curve for the flight path angle γ can then be obtained from (12), (13) and the speed tracking curve as shown in Figure 1. The resulting tracking curve for the flight path angle is as shown in Figure 2.

Similar to the discussion on (1), by analyzing (2), it is seen that γ cannot be directly controlled in the considered range of the climbing phase. In particular, between 166 and 200 s, $\dot{\gamma}$ is approximately $-0.12°$/s. The tracking curve for γ after time $t = 166$ s thus needs to be revised according to this value, as will be done in our simulation later.

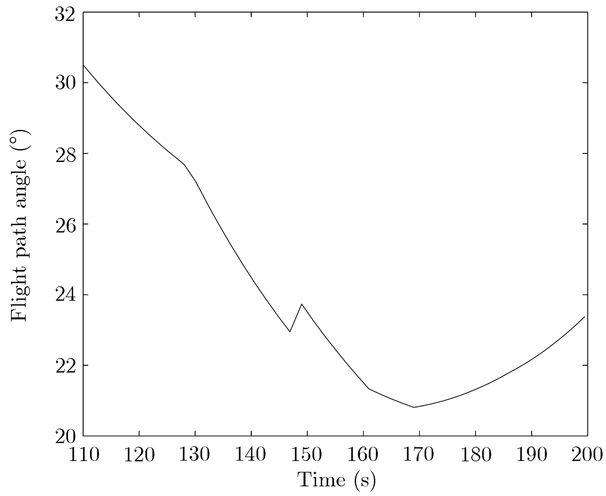

Figure 2 The tracking curve for the flight path angle γ.

3.3 Design of the tracking curves for the angle of attack

As observed before, the two long-period variables, the speed and the flight path angle, are not directly controllable at high altitude and high speed conditions and need to be controlled through the short-period variables, the angle of attack and the pitch rate. According to the practical requirements, we first make the pitch rate q track 0°/s and then design the tracking curve for the angle of attack in the following steps.

1. The angle of attack is between 5° and 10° [1,2], with the constraints on the overload and the stall out taken into account.

2. From (5) and $q = 0$, we obtain $\dot{\alpha} = -\dot{\gamma}$. Obtain the tracking curve for the angle of attack as follows: ascending by 5° from $t = 110$ s to $t = 160$ s and retaining at 10° between $t = 160$ s and $t = 200$ s.

The resulting tracking curve is as shown in Figure 3.

4 Design of the control law

In this section, a characteristic model based all-coefficient adaptive control law is designed for the two short-period variables, the angle of attack α and the pitch rate q. The design of this control law consists of three parts: characteristic modeling, parameter identification and all-coefficient adaptive control. We first construct the characteristic model

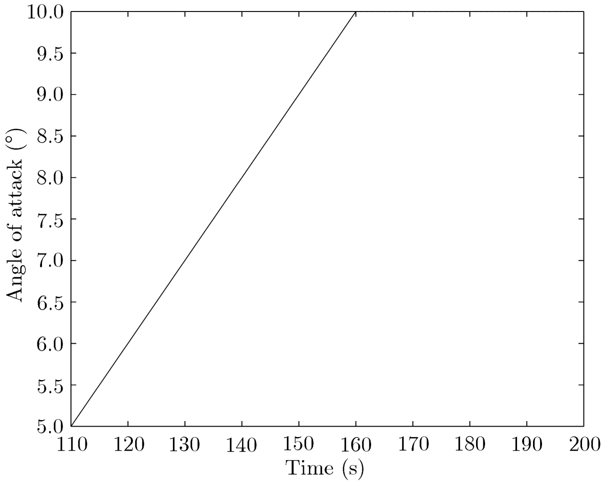

Figure 3 The tracking curve for the angle of attack α.

for the two short-period variables.

Theorem 4.1. With an appropriately selected sampling period, the short-period variables, the angle of attack α and the pitch rate q, of the vehicle satisfy the following characteristic model:

$$\begin{aligned}\alpha(k+2) &= f_{11}(k)\alpha(k+1) + f_{12}(k)\alpha(k) \\ &\quad + g_1(k)\overline{DE}, \qquad (14)\\ q(k+2) &= f_{21}(k)q(k+1) + f_{22}(k)q(k) \\ &\quad + g_2(k)\overline{DE}, \qquad (15)\end{aligned}$$

where $\overline{DE}$ is the degree of elevons, and $f_{ij}, i,j = 1,2$, and $g_i, i = 1,2$, satisfy (7).

Proof. Divide the time interval $[110, 200]$ into N sub-intervals $[t_i, t_{i+1}], i = 0, 1, \ldots, N-1$, not necessarily of equal length, with $t_0 = 110$ s and $t_N = 200$ s. Select a working point x_i within each interval $[t_i, t_{i+1}]$. Fix the time varying parameters nearby x_i at their values at x_i. Then, the following equations hold[13]:

$$\begin{aligned}&\ddot{\Delta}\alpha + a_{11}(x_i)\dot{\Delta}\alpha + a_{12}(x_i)\Delta\alpha \\ &\qquad = b_{11}(x_i)\Delta\dot{\overline{DE}} + b_{12}(x_i)\Delta\overline{DE}, \\ &\ddot{\Delta}q + a_{21}(x_i)\dot{\Delta}q + a_{22}(x_i)\Delta q \\ &\qquad = b_{21}(x_i)\Delta\dot{\overline{DE}} + b_{22}(x_i)\Delta\overline{DE},\end{aligned}$$

where $\Delta\alpha = \alpha(t) - \alpha(x_i)$, $\Delta q = q(t) - q(x_i)$, $\Delta\overline{DE} = \overline{DE}(t) - \overline{DE}(x_i)$, $t \in [t_i, t_{i+1}]$, and $a_{ij}(x_i)$ and $b_{ij}(x_i)$, $i,j = 1,2$, are constants. For a given time interval $[t_i, t_{i+1}]$ and the operation point x_i within it, it was shown in refs. [7, 8] that the following characteristic model can be obtained by appropriately selecting the sampling period $T(x_i)$:

$$\begin{aligned}\alpha(k+2) &= \bar{f}_{11}(x_i,k)\alpha(k+1) + \bar{f}_{12}(x_i,k)\alpha(k) \\ &\quad + \bar{g}_1(x_i,k)\overline{DE}, \\ q(k+2) &= \bar{f}_{21}(x_i,k)q(k+1) + \bar{f}_{22}(x_i,k)q(k) \\ &\quad + \bar{g}_2(x_i,k)\overline{DE},\end{aligned}$$

where $\bar{f}_{ij}, \bar{g}_i,\ i,j = 1,2$, satisfy (7). Select $T = \min_{1\leqslant i\leqslant N} T(x_i)$. Since (7) is satisfied by all $\bar{f}_{ij}$ and $\bar{g}_i$, the result of the theorem follows by representing $\bar{f}_{ij}(x_i,k)$ and $\bar{g}_i(x_i,k)$ as $f_{ij}(k)$ and $g_i(k)$.

With the dynamics of the short-period variables represented in the form of (14) and (15), the six parameters $f_{ij}(k)$ and $g_i(k)$ can be identified by using the least squares method and projection into (7). Let the identified parameters be denoted by $\hat{f}_{ij}(k)$, $i,j = 1,2$ and $\hat{g}_i(k)$, $i = 1,2$. Consequently, an all-coefficient adaptive control law can be designed as

$$\begin{aligned}\overline{DE} &= u_1 + u_2, \\ u_i &= u_{\mathrm{G}i} + u_{\mathrm{I}i},\ i = 1,2,\end{aligned}$$

and for $i = 1,2$,

$$\begin{aligned}u_{\mathrm{G}i}(k) &= -\frac{l_1\hat{f}_{i1}(k)e_i(k) + l_2\hat{f}_{i2}(k)e_i(k-1)}{\hat{g}_i(k)}, \\ u_{\mathrm{I}i}(k) &= u_{\mathrm{I}i}(k-1) - k_{\mathrm{I}i}e_i(k),\end{aligned}$$

where $l_1 = 0.382$, $l_2 = 0.618$, $e_1(k) = \alpha(k) - \alpha_{\mathrm{R}}(k)$ with α_{R} being the tracking curve for the angle of attack, $e_2(k) = q(k)$ and

$$k_{\mathrm{I}i} = \begin{cases} k_{\mathrm{I}1i}, & \text{if } e_i(k)(e_i(k) - e_i(k-1)) > 0, \\ k_{\mathrm{I}2i}, & \text{if } e_i(k)(e_i(k) - e_i(k-1)) \leqslant 0,\end{cases}$$

with $k_{\mathrm{I}1i} \gg k_{\mathrm{I}2i} > 0$ being some parameters to be adjusted.

5 Simulation results

In the simulation, $t_0 = 110$ s, $h_0 = 25$ km, $M_0 = 2.5$ Mach, $\alpha_0 = 5°$, $\gamma_0 = 28°$ and $\overline{DE}_0 = -12°$. The simulation results are shown in Figures 4–9.

From Figures 6 and 7, it is seen that the coordination control of the speed and altitude has been achieved. We next consider the effect of the overload on the closed-loop system. According to the following relationship:

$$n = \frac{L\cos\gamma + T\sin(\alpha+\gamma) - D\sin\gamma}{G},$$

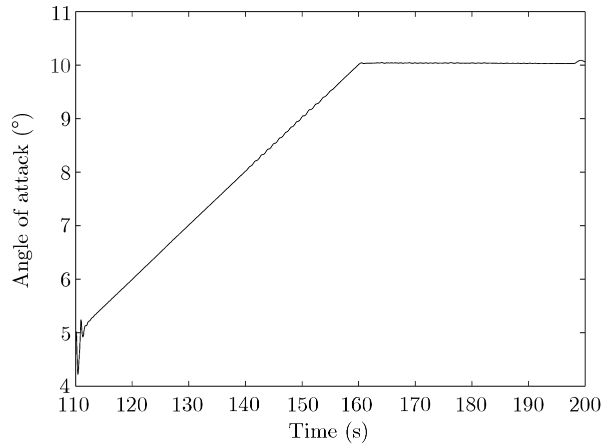

Figure 4 The tracking of the angle of attack α.

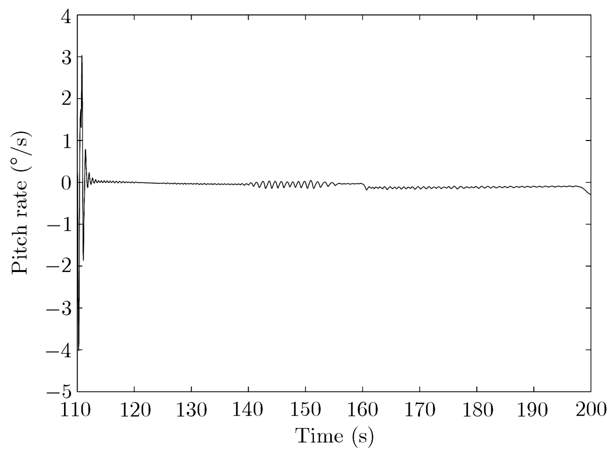

Figure 5 The tracking of the pitch rate q.

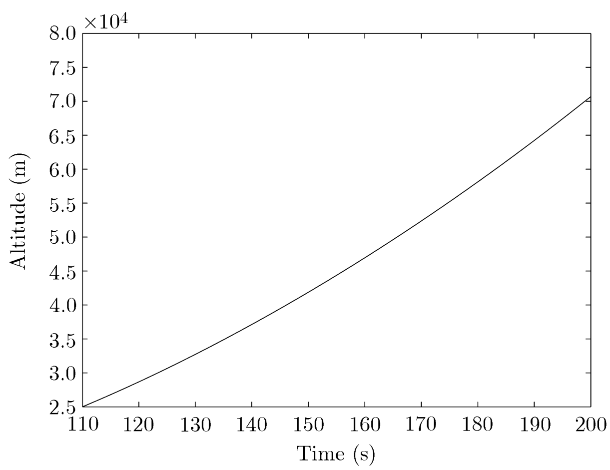

Figure 6 The altitude h.

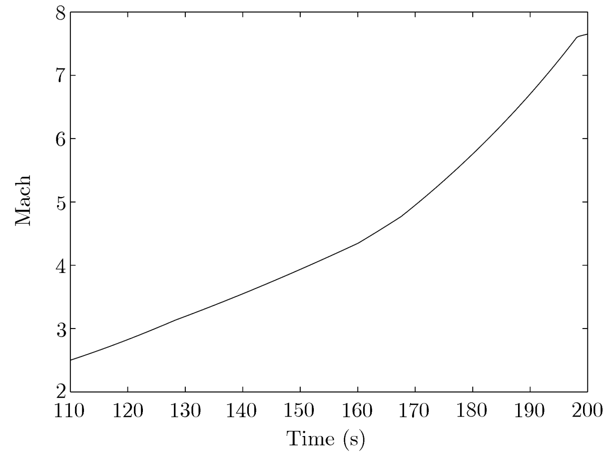

Figure 7 The speed V.

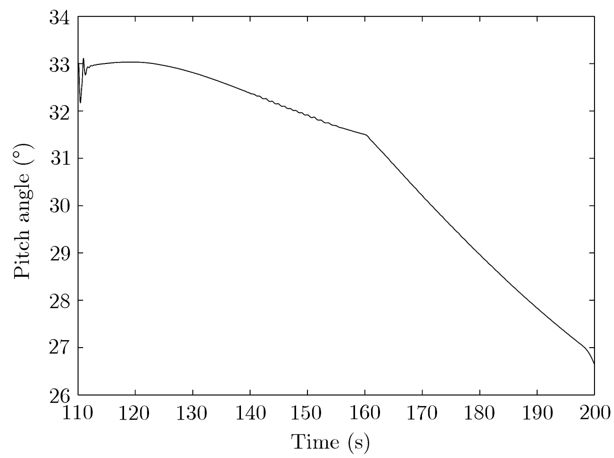

Figure 8 The pitch angle.

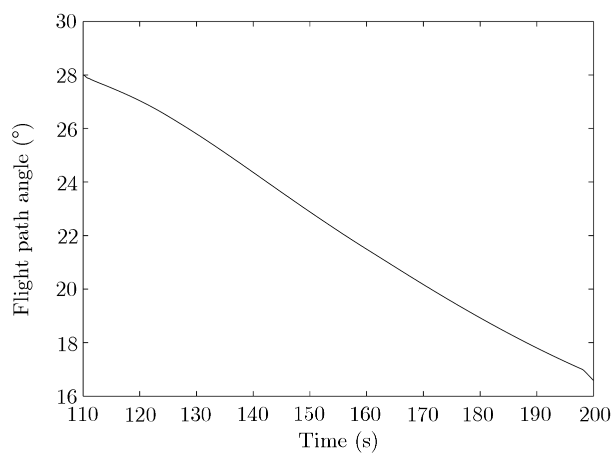

Figure 9 The flight path angle γ.

where n and G denote the overload and the weight of the vehicle respectively, we obtain the simulation result as shown in Figure 10.

The constraint is satisfied since the overload is less than 2. From the simulation results, we can also conclude that our simple control design realizes the coordination control of the altitude and the speed with the constraints of the pitch angle and overload.

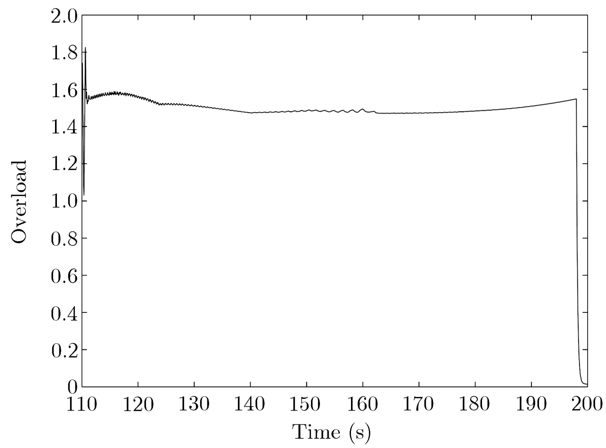

Figure 10 The effect of the overload.

The robustness of the control law against the initial values of the parameters has also been investigated by simulations. Multiple simulation runs were conducted with the initial values of the parameters being within the following range: $t_0 \in [109.1, 110.4]$ s, $M_0 \in [2, 2.9]$ Mach, $h_0 \in [23, 25.3]$ km, $\alpha_0 \in [4.8°, 5.2°]$, $\gamma_0 \in [20°, 29°]$, and $\overline{DE}_0 \in [-9°, -14°]$. The simulation results show a good tracking process with respect to the angle of attack and the pitch rate. The thrust experiences a sharp change at $t = 200$ s with a decrease from 240 kN to 0. With a longer simulation time, the control law works properly after $t = 200$ s.

Remark 5.1. There has been no report in the open literature on the climbing control problem of the X-34 vehicle at high altitude as examined in this paper. In this problem, due to the rapid change of the aerodynamic characteristics and the emergence of strong nonlinearity, the aerodynamic coefficients are difficult to express using the functions of the states. Thus, an analytic expression of the dynamic model, which is critical to the modern control methods, cannot be obtained. Multiple operation points are needed in the PID control approach for ordinary flight control. However, the above simulation results indicate that the characteristic model based all-coefficient adaptive control design is indeed capable of achieving the control objective without the need of multiple operation points.

6 Conclusions

The longitudinal climbing control design problem is considered for the trans-atmosphere vehicle X-34 with rapid changes of the speed, altitude, aerodynamic characteristics, mass, center of gravity and moment of inertia. By analyzing in detail the dynamic characteristics of the vehicle and the air dynamic data, the tracking curves for the angle of attack and the pitch rate, and characteristics of the short-period variables, an all-coefficient adaptive controller was designed, which achieves the control objective.

1 Pamadi B N, Brauckmann G J. Aerodynamic characteristics and development of the aerodynamic database of the X-34 reusable launch vehicle. In: Proc of the International Symposium on Atmospheric Reentry Vehicles and Systems, Arcachon, France, March 16–18, 1999
2 Pamadi B N, Brauckmann G J, Ruth M J, et al. Aerodynamic characteristics, database development and flight simulation of the X-34 vehicle. In: Proc of the 38th Aerospace Sciences Meeting & Exhibit, AIAA 2000-0900, Reno, NV, January 10–13, 2000
3 Zhou Y X, Zhang Z Y, Ming X. Conceptual study on trans-aerosphere flight control laws for a vehicle in climbing phase (in Chinese). Flight Dynam, 2006, 24(1): 9–12
4 Wu H X. All-coefficient Adaptive Control Theory and Application (in Chinese). Beijing: Defense Industry Press, 1990
5 Wu H X, Sa Z. An all-coefficients identification adaptive control method and its applications. In: Proc 10th IFAC World Congress, Munich, 1987
6 Hu J. All-coefficient adaptive reentry lifting control of manned spacecraft (in Chinese). J Astronaut, 1998, 19(1): 8–12
7 Meng B, Wu H X. Proof of the characteristic model of the linear time invariant systems (in Chinese). Sci China Ser F-Inf Sci, 2007, 37(10): 1258–1271
8 Wu H X, Hu J, Xie Y C. Characteristic model-based all-coefficients adaptive control method and its applications. IEEE Trans Syst Man Cybern, 2007, 37(2): 213–221
9 Xie Y C, Wu H X. Robustness of all-coefficient adaptive control (in Chinese). Acta Autom Sin, 1997, 3(2): 153–158
10 Dang Y, Mi J, Cheng Y. Principles and Applications of Global Navigation Satellite Systems (in Chinese). Beijing: Sino Maps Press, 2007. 30–31
11 Xiao Y L. Modeling of Aeronautics and Astronautics: Theoretical Foundation of Flight Dynamics (in Chinese). Beijing: Beijing University of Aeronautics and Astronautics Press, 2003.

38–51

12 Wu H X, Hu J, Xie Y. Characteristic Model-based Intelligent Adaptive Control (in Chinese). Beijing: Science and Technology Press of China, 2009

13 Wu S T, Fei Y H. Flight Control Systems (in Chinese). Beijing: Beijing University of Aeronautics and Astronautics Press, 2005. 46–103

Appendix Nomenclature

V	Velocity	$\overline{XCG}$	Position of center of gravity
h	Altitude	$\overline{CGREF}$	Reference center of gravity (10.668 m)
γ	Flight path angle	C_L	Lift coefficient
m	Mass	C_D	Drag coefficient
I_y	Moment of inertia	C_M	Pitching moment coefficient
P	Thrust	C_Z	Total aerodynamic coefficient in the Z direction of the body coordinate system
q	Pitch rate	$\overline{CLB}$	Basedline lift coefficient
α	Angle of attack	$\overline{CDB}$	Baseline drag coefficient
μ	Gravitational constant	$\overline{CMB}$	Baseline pitching moment coefficient
ω_E	Rotation rate of the Earth	$\overline{CLDE}$	Lift coefficient due to elevon deflection
R_E	Radius of the Earth, 6371386 m	$\overline{CDDE}$	Drag coefficient due to elevon deflection
M	Mach number	$\overline{CMDE}$	Pitching moment coefficient due to elevon deflection
L	Lift	$\overline{CLBF}$	Lift coefficient due to body flap deflections
D	Drag	$\overline{CDBF}$	Drag coefficient due to body flap deflection
M_y	Pitching moment	$\overline{CMBF}$	Pitching moment coefficient due to body flap deflection
ρ	Density of air	$\overline{CMQ}$	Pitching moment coefficient due to the pitch rate
n	Overload	A_0	The initial value of the variable A
G	Weight		
S	Reference area (33.2 m^2)		
$\bar{c}$	Mean aerodynamic chord (4.43 m)		